



## OPEN Fibroblast growth factor 23 neutralizing antibody partially rescues bone loss and increases hematocrit in sickle cell disease mice

Liping Xiao<sup>✉</sup>, Wei He & Marja M. Hurley<sup>✉</sup>

Fibroblast Growth Factor 23 (FGF23) is increased in serum of humanized Sickle Cell Disease (SCD) mice. Since FGF23 is associated with impaired bone formation, we examined the effect of FGF23-neutralizing antibody (FGF23Ab) on bone loss in SCD mice. Healthy control (Ctrl) and SCD 5-months-old female mice were treated with FGF23Ab or isotype-specific IgG for 6 weeks. Significantly reduced hematocrit in SCD mice was increased by FGF23Ab. MicroCT of SCD femurs revealed no significant reduction in metaphyseal bone volume/total volume vs. Ctrl mice. However, histomorphometry of SCD femur revealed significantly reduced mineral apposition rate, bone formation rate, inter-label thickness, and osteoid surface, which were increased by FGF23Ab. Significantly increased osteoclast number/bone perimeter in SCD mice was reduced by FGF23Ab. Bone marrow stromal cells (BMSC) cultured in osteogenic media revealed significantly reduced mineralized nodules in SCD-IgG-BMSC that was increased in SCD-FGF23Ab-BMSC. FGF23 and  $\alpha$ Klotho protein was significantly increased in SCD-IgG-BMSC and was not reduced by FGF23Ab. However, phosphorylated FGF Receptor-1, the receptor through which FGF23 signals, was significantly reduced by FGF23Ab. The mineralization inhibitor osteopontin was significantly increased in SCD-IgG-BMSC cultures and was reduced by FGF23Ab. We conclude that FGF23Ab may be efficacious in improving some parameters of reduced bone formation in female SCD mice.

**Keywords** FGF23 neutralizing antibody, Sickle cell bone disease, Hematocrit, Osteopontin

Sickle cell disease (SCD), the most common genetic hemoglobin disorder in humans, is an autosomal recessive inherited disease in which hemoglobin S (HbS) predominates because of the substitution of the amino acid glutamic acid with valine at position 6 of the beta-globin protein. The abnormal HbS polymerizes under conditions of dehydration or acidosis, resulting in sickling of red blood cells (RBCs) that reduces their survival and function. Complications include anemia, vaso-occlusion, and vasoconstriction<sup>1</sup>. SCD is associated with multi-organ damage including damage in bone where osteoporosis and osteopenia are common bone complications<sup>1,2</sup>. Approximately 80% of adults with SCD have low bone mineral density (BMD), but the underlying etiology linking SCD to reduced BMD is not fully defined in the absence of common risk factors such as age, gender, and menopausal status<sup>2</sup>. Among the contributing causes of low bone mass in SCD are delayed constitutional growth and maturation associated with insulin-like growth factor 1 (IGF1) deficiency, hypothyroidism, and micronutrient deficiencies<sup>1</sup>.

Studies have shown that bone marrow expansion from chronic anemia and increased erythropoiesis, impaired matrix mineralization from vitamin D deficiency, recurrent bone infarcts and vaso-occlusion, chronic inflammation, and sedentary lifestyle due to pain all contribute to development of osteoporosis in SCD<sup>3–5</sup>. Using the humanized sickle cell disease mouse models<sup>6</sup>, we<sup>7–9</sup> and others<sup>10,11</sup> have shown significant impairment of bone formation in SCD mice. However, the etiology is not fully defined.

Currently, there are no targeted therapies to prevent or treat compromised bone health in humans with SCD, and there are no consensus guidelines for the use of well-established anti-osteoporotic therapies in SCD patients<sup>5</sup> since potential adverse effects of these reagents limit their use in SCD patients. Furthermore, although

Division of Endocrinology and Metabolism, Department of Medicine, UConn Health School of Medicine, Farmington, CT 06030, USA. ✉email: xiao@uchc.edu; hurley@uchc.edu

two clinical trials using antiresorptive agents were initiated (NCT00639392 2008–2011 and NCT02972138c 2010–2017), one trial was withdrawn, and the second trial was published but did not report on the proposed outcomes or report in clinicaltrials.gov on the efficacy of antiresorptive agents in bone loss in SCD subjects.

Fibroblast growth factor 23 (FGF23) is an endocrine hormone that is mainly produced by osteocytes and osteoblasts (OB) in bone. FGF23 acts on the kidneys to regulate phosphate (Pi), vitamin D homeostasis, and bone mineralization<sup>12,13</sup>. FGF23 is upregulated in bone by a variety of factors including erythropoietin (EPO)<sup>14–16</sup>. FGF23 levels in blood are increased in chronic kidney disease patients and in several inherited hypophosphatemia rickets/osteomalacia disorders<sup>17</sup>. Limited studies have reported increased serum FGF23 in SCD subjects since the discovery of FGF23 in 2000<sup>18–20</sup>. However, there are limited studies on the associations of FGF23 and bone loss in SCD subjects<sup>21</sup>. We previously published a significantly reduced bone mass in SCD mice<sup>7,9</sup> was associated with reduced OB terminal differentiation marker gene expression. Our study<sup>22</sup> and other studies have shown that FGF23 is associated with impaired bone mineralization and bone formation<sup>23–25</sup>. Of relevance, FGF23-neutralizing antibody has been utilized to increase bone formation in the Hyp mouse model of the genetic disorder X-linked hypophosphatemia (XLH) with increased FGF23 production in bone demonstrating improved histomorphometry measures of osteomalacia<sup>26</sup>.

While traditionally considered to be mainly produced by osteocytes within bone, research has shown that erythroblasts, the precursor cells to red blood cells, can produce FGF23, particularly in situations of hypoxia within the bone marrow and often triggered by the administration of granulocyte colony-stimulating factor (G-CSF) which is used to mobilize hematopoietic stem cells. This FGF-23 production by erythroblasts plays a role in facilitating the release of these stem cells from the bone marrow by suppressing their adhesion mechanisms<sup>27</sup>. Interestingly, Weidner et al. reported that increased FGF23 levels are linked to ineffective erythropoiesis and impaired bone mineralization in myelodysplastic syndromes and is modulated by FGF23Ab<sup>28</sup>. Studies by Roissant et al. reported that mice with chronic kidney disease (CKD) or pneumonia had increased serum FGF23, and an FGF23 antibody prolonged survival<sup>29</sup>. Of note, the FGF23Ab used in the present study obtained from Amgen was also used in these other preclinical mouse models of anemia, myelodysplastic syndromes<sup>28</sup>, and CKD<sup>29</sup>. In addition, it should be noted that another FGF23Ab is FDA-approved for the treatment of phosphate wasting and osteomalacia in human rickets and in humans with XLH<sup>30</sup>.

Since preclinical murine models of disorders with increased FGF23 discussed above reported efficacy of FGF23Ab, and our previously published studies demonstrated increased serum FGF23 and impaired bone formation in mandibular dento-alveolar<sup>22</sup> and femoral bones<sup>31</sup> of high molecular weight FGF2 transgenic mice that could be rescued using an FGF23 neutralizing antibody (FGF23Ab)<sup>22,31</sup>, we examined the effect of this FGF23Ab on bone loss in female SCD mice.

Although curative therapy for SCD such as hematopoietic stem cell transplant is available, previous studies have reported only a 15% bone-marrow-donor-to-bone-marrow-recipient match rate<sup>32</sup>. Other recently FDA-approved genetic therapies include Casgevy (exagamglogene Autotemcel) which increases fetal Hb<sup>33</sup> and Lyfgenia (Lovotibeglogene autemcel)<sup>34</sup> which is a modified HbA<sup>T87Q</sup>; these are now available although Lyfgenia's associated malignancies have been reported<sup>35</sup>. The cost of these therapies in addition to limited accessibility may prohibit their wide use in the short term, thus the need for other treatments for SCD bone loss remains an unmet need.

## Materials and methods

### Experimental mice

Healthy control and Townes sickle cell disease female mice<sup>6</sup> on a mixed C57BL/6 and 129 genetic backgrounds were purchased from The Jackson Laboratory (Stock number: 013071, Bar Harbor, Maine, USA) and housed in the Center for Comparative Medicine at UConn Health for this study. All mice were fed with Envigo Teklad Diet-2918, which contains 1% calcium, 0.7% total phosphate, and 1.5 IU D3/g of diet. Healthy Control and SCD 5-months-old female mice were subcutaneously injected with FGF23Ab or isotype-specific IgG (10 mg/kg, 2 days/week) for 6 weeks. Then mice were sacrificed with CO<sub>2</sub> for sample collection. The control IgG or a rat anti-rat FGF23Ab (clone 58.5) were a gift from Amgen, Inc. (Thousand Oaks, CA). All animal protocols were approved by the UConn Health Institutional Animal Care and Use Committee. All experiments were performed in accordance with relevant guidelines and regulations. Additionally, the studies complied with the recommendations in the ARRIVE guidelines.

**End points:** Detailed information about methods, antibodies, ELISA kits, and primers is provided online in the Supplementary Methods and Supplemental Tables 1 and 2.

### Statistical analysis

Statistical analyses were done using SPSS and p values were calculated using a two-way ANOVA with Tukey's post hoc analysis. The results were considered significantly different at  $p < 0.05$ . GraphPad Prism 10 software was used to generate bar graphs showing individual values, with mean and standard error of the mean.

## Results

### Effect of FGF23Ab on blood hematocrit, serum erythropoietin, ferritin, intact and C-terminal FGF23

Hematocrit was significantly decreased in SCD mice compared with healthy control (Ctrl) mice and was significantly increased by FGF23Ab (Fig. 1A). Since erythropoietin (EPO) production by the kidney is increased in response to hypoxia and anemia<sup>36</sup>, we also measured serum levels of EPO. As shown in (Fig. 1B), EPO was significantly increased in SCD-IgG and was further significantly increased in FGF23Ab-treated SCD mice. Increased ferritin, a marker of excess iron or heightened inflammation, has been reported in SCD<sup>1</sup> and was also

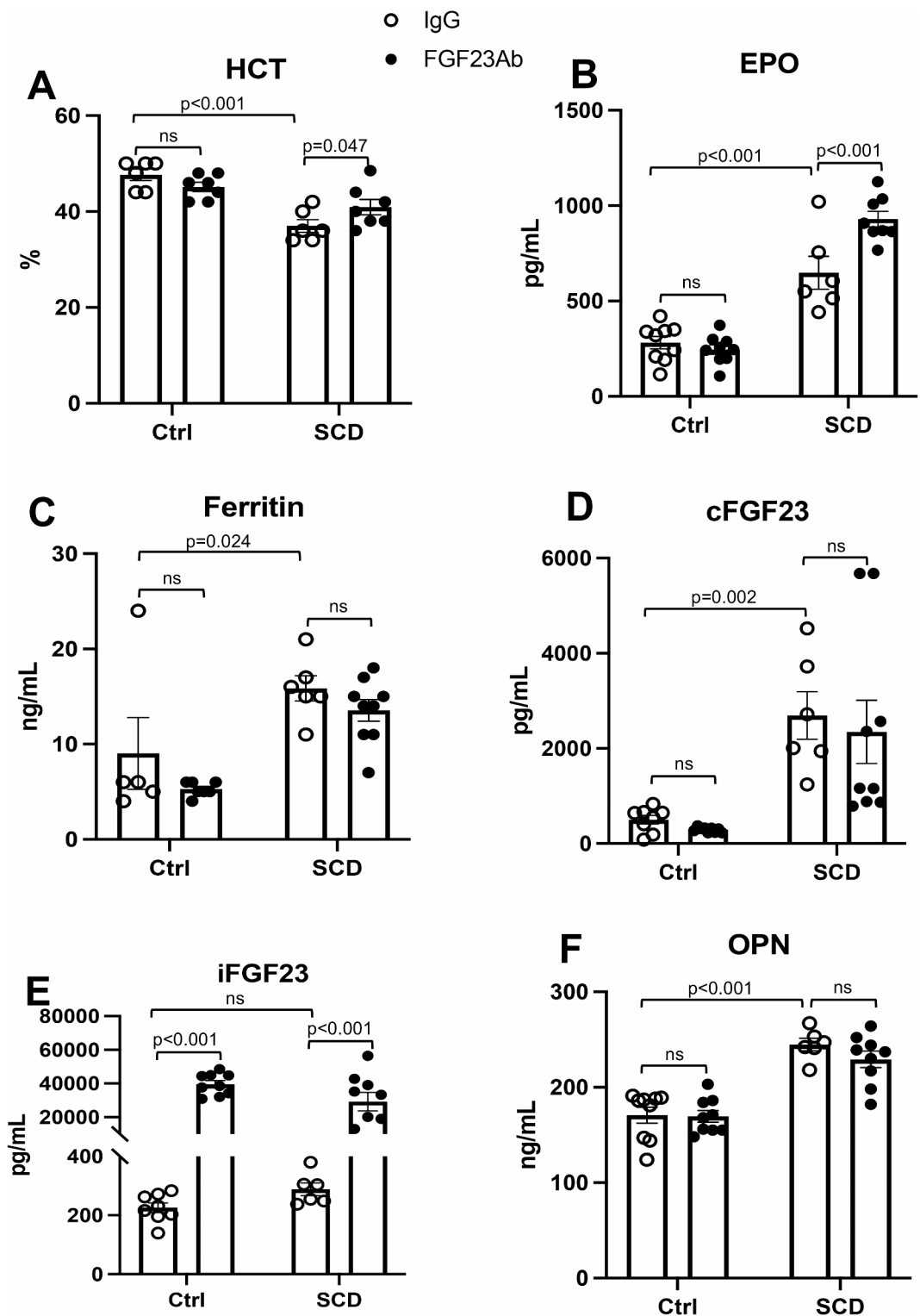


**Fig. 1.** Hematocrit, serum EPO, ferritin, iFGF23, cFGF23, and osteopontin from Ctrl and SCD female mice treated with IgG or FGF23Ab. Five-month-old Ctrl and SCD female mice were sq injected with IgG or FGF23Ab 2 times per week for 6 weeks. (A) HCT,  $n = 6-7$  mice/group; (B) serum EPO,  $n = 6-9$  mice/group; (C) serum Ferritin,  $n = 5-9$  mice/group; (D) serum cFGF23,  $n = 6-9$  mice/group; (E) serum iFGF23,  $n = 6-9$  mice/group; (F) serum Osteopontin,  $n = 6-9$  mice/group. Data are shown as individual values, with mean and standard error of the mean.

reported to inhibit calcification in human OB cultures in a dose-dependent manner<sup>37</sup>. We therefore measured its expression in serum of Ctrl and SCD mice. As shown in Fig. 1C, serum ferritin was significantly increased in IgG-treated SCD mice but was not modulated by FGF23Ab. Since FGF23 can negatively regulate erythropoiesis, we measured total FGF23 levels, including total c-terminal FGF23 level, and intact iFGF23. Compared with IgG-treated Ctrl mice, serum c-FGF23 was significantly increased in SCD-IgG mice (Fig. 1D) but was not significantly reduced by FGF23Ab. Serum iFGF23 (Fig. 1E) was not significantly increased in SCD-IgG mice but was significantly increased by FGF23Ab in both Ctrl and SCD mice. Since Osteopontin was reported to be regulated by FGF23 (35), we measured its serum levels. As shown in Fig. 1F, osteopontin was significantly increased in SCD-IgG but was not significantly decreased by FGF23Ab.

Dual-energy X-ray absorptiometry (DXA) analysis of the effect of FGF23Ab on bone density in SCD female mice

Bone mineral density (BMD) and bone mineral content (BMC) were assessed in femurs of Ctrl-IgG, Ctrl-FGF23Ab, SCD-IgG and SCD-FGF23Ab mice. Compared with Ctrl-IgG, there was a significant reduction in BMC (Table 1) in femurs of SCD-IgG mice that was not rescued by FGF23Ab. Femur BMD in SCD was also significantly decreased (Table 1) and was not increased by FGF23Ab.

Effect of FGF23Ab on structural parameters of femur metaphysis and diaphyseal cortex in SCD female mice

We examined the effects of FGF23Ab on bone micro-architecture in SCD mice by **micro-computed tomography (microCT)**. Quantitative microCT structural analysis of femur metaphyseal trabeculae (Table 1) revealed no significant reduction in femur metaphyseal bone volume/total volume (BV/TV), trabecular number (Tb.N), trabecular thickness (Tb.Th), or trabecular spacing (Tb.Sp) in SCD-IgG versus Ctrl-IgG mice. FGF23Ab treatment did not alter these parameters in SCD mice.

The effect of FGF23Ab on diaphyseal cortex of SCD mice was also determined. Quantitative analysis (Table 1) shows no significant differences in total area (Tt.Ar) between Ctrl-IgG and SCD-IgG; however, significantly reduced cortical area (Ct.Ar), and cortical area/total area (Ct.Ar/Tt.Ar) and significantly increased marrow area (Ma.Ar) and significantly decreased cortical thickness (Ct.Th) and BMD in SCD mice were not altered by FGF23Ab treatment.

Effect of FGF23Ab on histomorphometric parameters of bone formation in SCD female mice

Dynamic bone histomorphometric analysis of femur metaphysis and representative images showed that there was decreased double-labeling distance in SCD-IgG which was increased by FGF23Ab (Fig. 2A, SupFig. 1). Quantitative analysis, as shown in Fig. 2B, of mineralized surface/bone surface (MS/BS) was markedly reduced in SCD-IgG and was increased by FGF23Ab but not significantly. However, as shown in Figs. 2C–E, there was significantly decreased mineral apposition rate (MAR), bone formation rate (BFR/BS), and inter-label thickness (Ir.LTh) in the SCD-IgG group vs. the Ctrl-IgG group, and FGF23Ab significantly increased MAR, BFR/BS, and Ir.L.Th in SCD. Static bone histomorphometry analysis showed that there was significantly decreased osteoblast surface per bone surface (Obs/BS) and osteoid surface per bone surface (OS/BS) in the SCD-IgG group, and FGF23Ab treatment significantly increased OS/BS in SCD mice (Fig. 2F and G, SupFig.2). FGF23Ab significantly increased MAR (indicative of the individual activity of osteoblasts) and OS/BS, but not Obs/BS, suggesting FGF23Ab treatment improved function of individual osteoblasts to synthesize and deposit organic bone matrix (osteoid) proteins and initiate the mineralization of the matrix.

	Ctrl-IgG	Ctrl-FGF23Ab	SCD-IgG	SCD-FGF23Ab
DXA analysis of femur				
BMC (g)	0.0274 ± 0.0013	0.0279 ± 0.0002	0.0237 ± 0.0004 <sup>a</sup>	0.0237 ± 0.0010
BMD (mg/cm <sup>2</sup> )	76.17 ± 2.24	73.28 ± 1.68	68.37 ± 2.46 <sup>a</sup>	64.49 ± 1.87
MicroCT analysis of femoral metaphysis				
BV/TV (%)	4.87 ± 0.66	5.37 ± 0.56	5.21 ± 0.71	7.04 ± 0.71
Tb.N (1/mm)	2.67 ± 0.08	2.77 ± 0.07	2.88 ± 0.16	3.19 ± 0.18
Tb.Th (um)	47.09 ± 1.76	48.53 ± 1.31	49.45 ± 2.12	49.58 ± 1.03
Tb.Sp (um)	374.70 ± 11.20	360.22 ± 9.09	352.40 ± 23.07	321.28 ± 22.39
MicroCT analysis of femoral cortical bone				
Tt.Ar (mm <sup>2</sup> )	1.76 ± 0.07	1.80 ± 0.02	1.92 ± 0.06	1.94 ± 0.05
Ct.Ar (mm <sup>2</sup> )	0.82 ± 0.03	0.86 ± 0.01	0.73 ± 0.01 <sup>a</sup>	0.74 ± 0.02
Ct.Ar/Tt.Ar (%)	46.89 ± 0.54	48.00 ± 0.66	38.39 ± 1.13 <sup>a</sup>	38.0 4 ± 0.64
Ma.Ar (mm <sup>2</sup> )	0.93 ± 0.04	0.93 ± 0.02	1.18 ± 0.06 <sup>a</sup>	1.20 ± 0.03
Ct.Th (mm)	0.202 ± 0.004	0.212 ± 0.003 <sup>b</sup>	0.168 ± 0.005 <sup>a</sup>	0.165 ± 0.004
BMD (mg/ccm HA)	1333 ± 4	1347 ± 3 <sup>b</sup>	1311 ± 2 <sup>a</sup>	1307 ± 6

**Table 1.** DXA and MicroCT analysis of femur. Data are mean ± SE, *n* = 6–9 mice/group. a: Ctrl-IgG vs. SCD-IgG *p* < 0.05; b: Ctrl-IgG vs. Ctrl-FGF23Ab *p* < 0.05; *p* values were calculated using a two-way ANOVA with Tukey’s post hoc analysis.



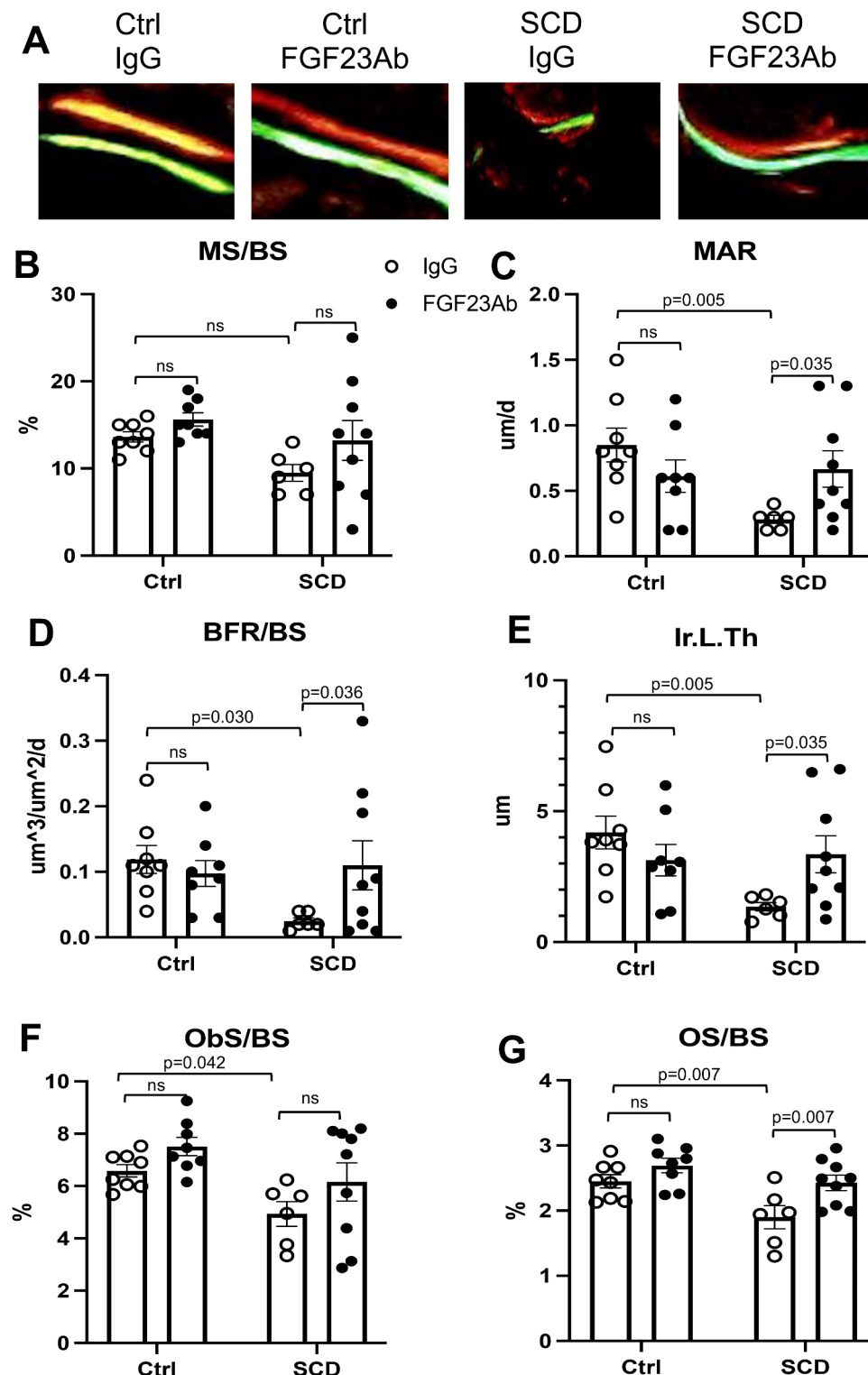


**Fig. 2.** Effect of FGF23Ab on bone histomorphometry parameters of femurs from Ctrl and SCD female mice. (A) Representative image of calcein/xylitol orange double labeling in femur. Analysis of (B) mineralization surface/bone surface (MS/BS), (C) mineral apposition rate (MAR), (D) bone formation rate (BFR/BS), (E) inter-label thickness (Ir.L.Th), (F) osteoblast surface/bone surface (ObS/BS), (G) osteoid surface/bone surface (OS/BS);  $n = 6-9$  mice/group. Data are shown as individual values, with mean and standard error of the mean.

### Effect of FGF23Ab on mineralized trabeculae and osteopontin (OPN) expression in SCD mice

We determined by histology the effect of FGF23Ab on mineralized femur trabeculae in SCD mice. As shown in Fig. 3A and C, von Kossa staining of femurs from Ctrl and SCD female mice showed no differences in mineralized trabeculae in Ctrl-IgG versus SCD-IgG mice; however, quantitative analysis showed that FGF23Ab markedly increased trabeculae spicule number in SCD bone. IHC staining and quantification showed that OPN staining intensity was markedly increased in osteoblast on the bone surface of SCD-IgG compared to Ctrl-IgG group; this was significantly reduced by FGF23Ab (Fig. 3B, D).

### Effect of FGF23Ab on histomorphometry parameters of osteoclast in femur of SCD mice

Since previous studies reported that decreased bone mass in SCD could be due in part to increased bone resorption<sup>10</sup>, we examined the effect of FGF23Ab on osteoclast parameters in femur metaphyseal bone from Ctrl and SCD mice. Representative images show more tartrate-resistant acid phosphatase (TRAP)-positive osteoclasts (arrows) in the SCD-IgG group compared to Ctrl-IgG which was reduced by FGF23Ab treatment (Fig. 4A, Sup. Figure 3). Static bone histomorphometry showed that osteoclast surface/bone surface (Oc.S/BS) (Fig. 4B), osteoclast number/bone perimeter (N.Oc/B.Pm) (Fig. 4C), and osteoclasts number/total area (N.Oc/T.Ar) (Fig. 4D) were significantly higher in SCD-IgG group vs. Ctrl-IgG. FGF23Ab significantly decreased N.Oc/B.Pm in SCD-FGF23Ab group.

### Effect of FGF23Ab on bone-related gene expression in SCD female mice

Since histomorphometry showed impaired bone formation parameters and bone resorption parameters in SCD female mice, we examined the effect of FGF23Ab on osteoblast-, osteocyte-, and osteoclast-related gene expression in whole tibias from Ctrl and SCD female mice. As shown in Supplemental Table 3, in SCD-IgG versus Ctrl-IgG bones, mRNA for osteoblast-related gene Runx2 was significantly increased ( $p=0.017$ ), and Ocn was significantly decreased ( $p=0.011$ ) in SCD-IgG but not modulated by FGF23Ab. Based on genotype and treatment, there were no significant differences in Col1a1, tissue nonspecific alkaline phosphatase, or osteonectin mRNA (data not shown). Mineralization-related genes Mepe ( $p=0.047$ ) and Phex ( $p=0.028$ ) was significantly decreased and was not increased by FGF23Ab. Dmp1 mRNA was decreased but not significantly in SCD-IgG. Pyrophosphate-related gene Enpp1 was markedly but not significantly increased ( $p=0.097$ ) and was markedly reduced by FGF23Ab ( $p=0.059$ ). Osteocyte-related genes E11/gp38 ( $p=0.029$ ) and Opg mRNAs ( $p=0.01$ ) were significantly increased in SCD-IgG but were not reduced by FGF23Ab.

Also shown in Supplemental Table 3, we observed in SCD-IgG significantly reduced mRNAs for osteoclast (OCL)-related-genes Trap ( $p=0.023$ ) and Ctsk ( $p=0.051$ ) relative to Ctrl-IgG. As shown in Supplemental Table 3, Rankl/Opg ratio was similar among all 4 groups based on genotype and treatment. Other OCL genes Nfatc1 ( $p=0.077$ ), Ppargc1b ( $p=0.072$ ), and Slc40a1 ( $p=0.058$ ), and antioxidant-system-related gene Prxd2 ( $p=0.085$ ) were markedly increased but were not modulated by FGF23Ab. The inflammatory- and hypoxia-related gene Hif1a was significantly increased ( $p=0.012$ ) but was not reduced by FGF23Ab. Although Hif2a was not significantly increased in SCD-IgG bones, its expression was significantly decreased by FGF23Ab ( $p=0.032$ ).

The expression of genes involved in FGF23 regulation was also determined. As shown in Supplemental Table 3, in SCD-IgG, there was no significant increase in Galnt3 mRNA ( $p=0.098$ ). Galnt3 is the enzyme that glycosylates FGF23 and protects it from cleavage or modulation by FGF23Ab. However, the mRNA for Fam20c that promotes FGF23 proteolytic cleavage was significantly increased ( $p=0.04$ ) in SCD-IgG and was significantly decreased ( $p=0.029$ ) by FGF23Ab. Furin mRNA was markedly increased ( $p=0.083$ ) in SCD-IgG and was significantly reduced ( $p=0.019$ ) by FGF23Ab.

### Effect of FGF23-blocking antibody on serum markers of bone homeostasis

Serum parameters are shown in Table 2. Serum calcium was significantly decreased in SCD-IgG ( $p=0.04$ ) and was increased but not significantly by FGF23Ab. Serum phosphate levels were similar in Ctrl and SCD mice treated with IgG or FGF23Ab. Serum 25(OH)VitD, which is often decreased in SCD and can contribute to impaired bone formation, was significantly increased in SCD-IgG ( $p=0.001$ ) and was significantly reduced by FGF23Ab ( $p=0.014$ ). FGF23Ab significantly reduced 1,25(OH)<sub>2</sub>VitD ( $p=0.031$ ) and PTH ( $p=0.002$ ) in serum of Ctrl but not SCD mice. However, PTH was significantly reduced in SCD-IgG but was not significantly increased by FGF23Ab. Serum bone formation marker osteocalcin was significantly reduced in SCD-IgG and was not increased by FGF23Ab. However, PINP was similar in all groups based on genotype and treatment. Serum bone resorption marker CTX-1 was similar in Ctrl-IgG and SCD-IgG mice but FGF23Ab treatment significantly increased serum CTX-1 in SCD mice.

### Effect of FGF23Ab on mineralized bone nodule formation in bone marrow stem cell (BMSC) cultures from SCD female mice

We assessed whether bone nodule formation was decreased in BMSC cultures from SCD mice and whether FGF23 blocking antibody could modulate bone nodule formation in vitro. As shown by representative Alizarin-red staining for calcium (Fig. 5A) and quantitation of extracted Alizarin red (Fig. 5B), there were significantly lower concentrations in SCD-IgG cultures that were significantly increased by FGF23Ab.

Since FGF23 signals via FGFR1, we measured FGF23 and phosphorylated FGF Receptor-1 protein expression in 21-day BSMC cultures by Western blot. FGF23 protein and aKlotho (a co-receptor for FGF23) protein were significantly increased in SCD-IgG BMSC cultures compared with Ctrl-IgG (Fig. 5C and D) but was not significantly decreased by FGF23Ab. Phosphorylated FGFR1 was not significantly increased in SCD-IgG BMSC cultures but was significantly reduced by FGF23Ab (Fig. 5E). Since our in vivo studies showed that serum osteopontin was significantly increased in SCD-IgG (Fig. 1F) and osteopontin is associated with reduced bone formation and increased bone resorption<sup>38</sup>, we also measured its expression by western blot. As shown in

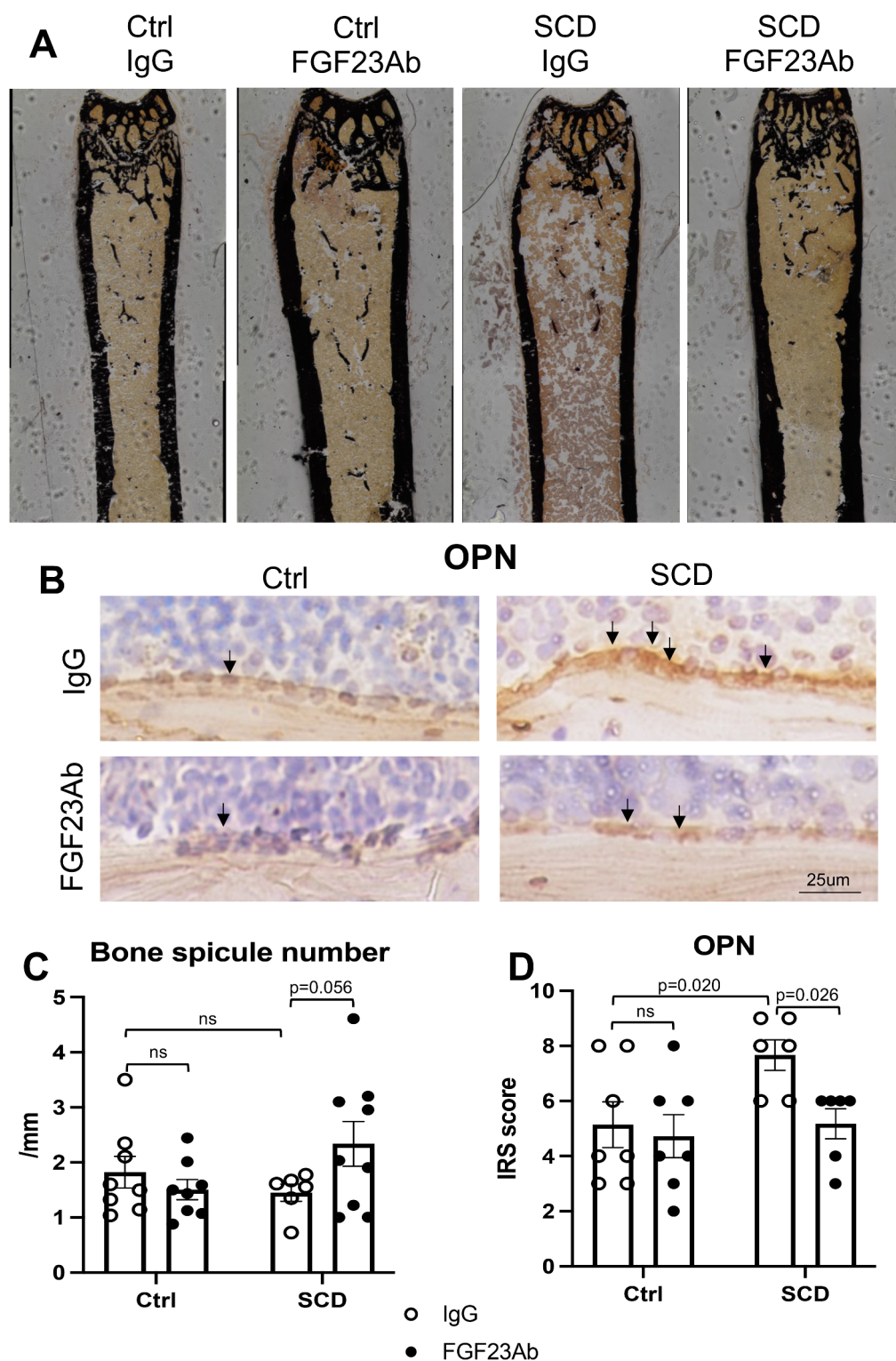


**Fig. 3.** Effect of FGF23Ab on bone mineralization and OPN level of femurs from Ctrl and SCD female mice. (A) Von Kossa staining and (C) quantification of femurs from Ctrl and SCD mice showed similar mineralized trabeculae in Ctrl-IgG and SCD-IgG treated mice. There was a markedly increased bone spicule number in SCD-FGF23Ab femurs. (B) OPN IHC staining and (D) quantification showed OPN intensity was significantly increased in osteoblast (arrows) on the bone surface of SCD-IgG compared to Ctrl-IgG group, that was partially rescued by FGF23Ab. Osteoblasts are identified as cuboidal cells that are located on the surface of bones.  $n = 6-9$  mice/group. Data are shown as individual values, with mean and standard error of the mean.



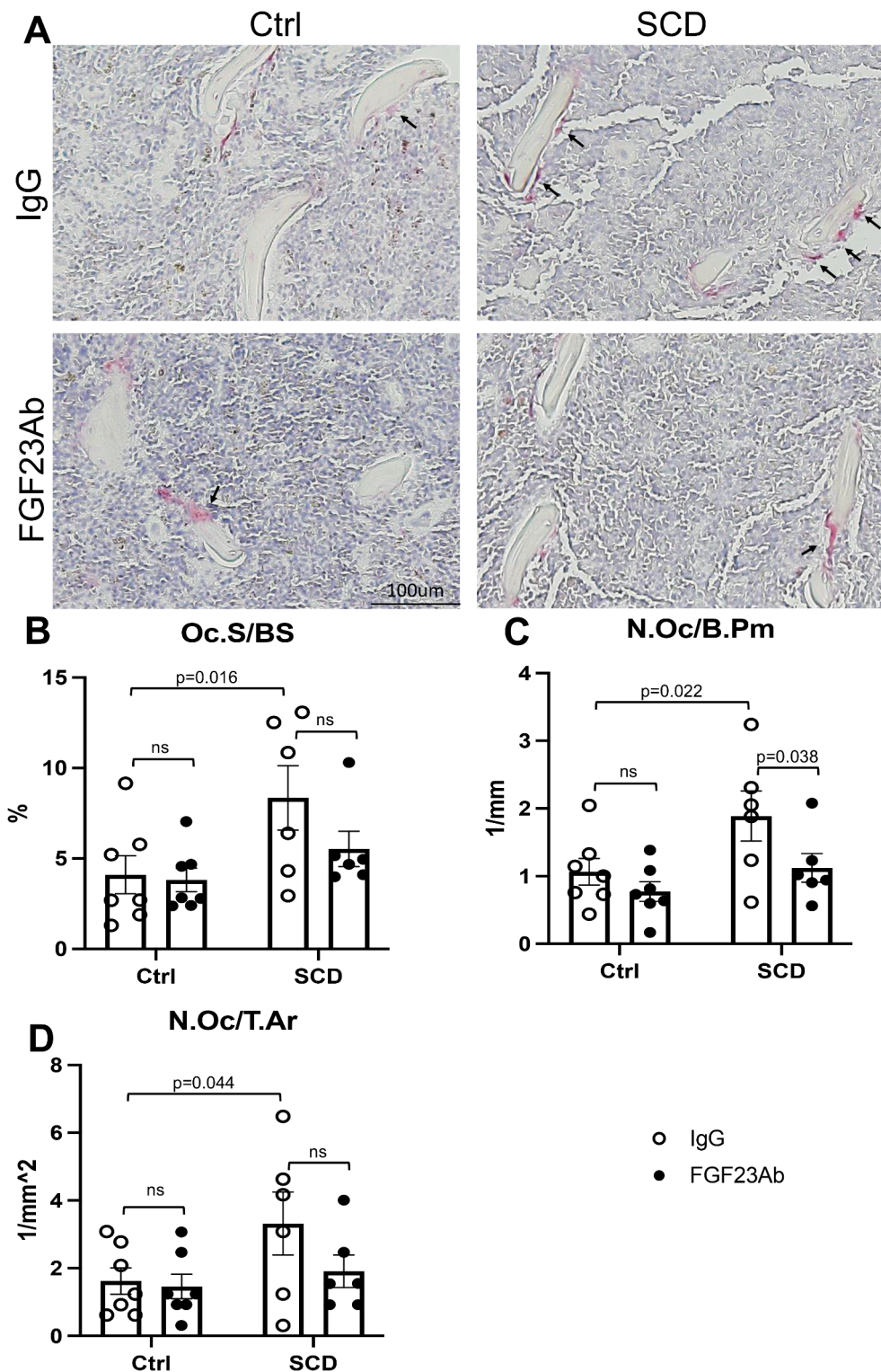


**Fig. 4.** Effect of FGF23Ab on TRAP staining and static histomorphometry of femurs from Ctrl and SCD female mice. (A) Representative image of TRAP-stained femurs. Static bone histomorphometry analysis of femur metaphysis, (B) osteoclast surface/bone surface (Oc.S/BS), (C) osteoclast number/bone perimeter (N.Oc/Pm), (D) osteoclast number/total area (N.Oc/T.Ar).  $n = 5-8$  mice/group. Data are shown as individual values, with mean and standard error of the mean.

	Ctrl-IgG	Ctrl-FGF23Ab	SCD-IgG	SCD-FGF23Ab
Calcium (mg/dL)	9.45 ± 0.35	9.10 ± 0.10	8.74 ± 0.13 <sup>a</sup>	9.10 ± 0.10
Phosphorus (mg/dL)	9.92 ± 0.21	10.17 ± 0.32	9.68 ± 0.16	10.29 ± 0.23
BUN (mg/dL)	18.9 ± 1.3	11.2 ± 1.3	19.9 ± 4.8	19.9 ± 1.8
Creatinine (mg/dL)	0.23 ± 0.02	0.31 ± 0.02	0.27 ± 0.02	0.25 ± 0.01
25(OH)D (ng/mL)	41.11 ± 2.94	42.89 ± 2.43	58.42 ± 2.08 <sup>a</sup>	48.83 ± 1.59 <sup>c</sup>
1,25(OH)2D (pmol/L)	115.00 ± 15.83	69.25 ± 11.12 <sup>b</sup>	113.67 ± 19.72	89.11 ± 11.69
PTH (pg/mL)	150.21 ± 30.52	54.77 ± 8.58 <sup>b</sup>	58.77 ± 4.20 <sup>a</sup>	78.63 ± 13.98
Osteocalcin (ng/mL)	57.55 ± 6.51	59.56 ± 5.45	37.45 ± 3.71 <sup>a</sup>	34.36 ± 1.76
PINP (ng/mL)	24.38 ± 2.83	26.81 ± 1.99	20.13 ± 2.42	22.03 ± 2.17
CTX-1 (ng/mL)	9.85 ± 0.97	8.79 ± 0.87	7.72 ± 0.49	13.20 ± 1.29 <sup>c</sup>

**Table 2.** Serum bone markers. Data are mean ± SE,  $n = 6-9$  mice/group. a: Ctrl-IgG vs. SCD-IgG  $p < 0.05$ ; b: Ctrl-IgG vs. Ctrl-FGF23Ab  $p < 0.05$ ; c: SCD-IgG vs. SCD-FGF23Ab  $p < 0.05$ .  $p$  values were calculated using a two-way ANOVA with Tukey's post hoc analysis.

Fig. 5F osteopontin protein was significantly increased in SCD-IgG BMSC cultures compared with Ctrl-IgG, and FGF23Ab significantly reduced osteopontin in SCD-BMSC cultures.

## Discussion

In this study, we utilized the humanized SCD mouse that phenocopies human SCD, including systemic organ damage due to vaso-occlusion and hemolytic anemia. We used this mouse to characterize the effect of FGF23-neutralizing antibody on bone loss we previously reported in female SCD mice<sup>7</sup>. Since FGF23 is associated with impaired bone formation, we measured both iFGF23 and cFGF23 (total FGF23) in serum. Serum cFGF23 was significantly higher in SCD mice which was not altered by FGF23Ab treatment. After the treatment with FGF23Ab, the iFGF23 levels were increased in both Ctrl and SCD mice. However, interpretation of serum iFGF23 levels in the presence of FGF23Ab treatment is difficult since the markedly increased levels most likely reflects cross-reactivity with FGF23Ab in the assay. We previously reported decreased bone mass in both male and female SCD mice<sup>7,9</sup>; however, in this study we focused on female mice, which is a limitation of this study.

We confirmed anemia in SCD mice by demonstrating a significant reduction in HCT. Anemia in SCD is multi-factorial, and includes hemolysis, ineffective erythropoiesis, insufficient EPO responsiveness, and low oxygen affinity<sup>39,40</sup>. We observed significantly increased serum EPO, the major hormone produced by the kidneys in response to anemia, which stimulates the bone marrow to produce erythroid cells. Studies have reported that although circulating EPO is elevated in SCD, the amount is often relatively low for the degree of anemia<sup>41-43</sup>. Of relevance, it has been reported that high FGF23 levels inhibit renal EPO production in wild type mice and serum EPO concentrations<sup>41,44</sup>, and FGF23-blocking peptide increases serum EPO concentrations<sup>41</sup>. Given these reports of FGF23 modulation of EPO and our observation of significantly increased serum FGF23 in SCD-IgG mice, we posited that increased FGF23 could dampen EPO production by the kidney. In support of this possibility, we observed a further significant increase in serum EPO in SCD mice treated with FGF23Ab consistent with FGF23 being an inhibitor of EPO production by the kidney<sup>41</sup>. Since FGF23 is known to negatively affect erythropoiesis<sup>41</sup> and thus may further contribute to anemia in SCD, we speculate that the significantly increased HCT observed in SCD mice treated with FGF23Ab relieves its block on kidney production of EPO, resulting in significantly increased serum EPO thereby increasing erythropoiesis<sup>41</sup>.

Another common finding in SCD is iron overload<sup>45</sup>, and since iron decreases mineralization by iron-induced upregulation of ferritin<sup>37</sup>, we measured its expression in serum of Ctrl and SCD mice. We observed significant increase in serum ferritin in SCD-IgG which was not reduced in SCD-FGF23-Ab mice.

As shown in Table 2, serum PTH was lower in the SCD-IgG than Control-IgG mice. However, their serum 1,25(OH)2D levels are essentially the same. These data are noteworthy since high ferritin level can indirectly lead to an increase in 1-alpha hydroxylase activity, the enzyme responsible for activating vitamin D, by potentially influencing the body's need for calcium and thereby stimulating PTH secretion, which in turn activates 1-alpha hydroxylase in the kidneys. Essentially, when iron stores are high, the body may signal a need for more calcium absorption, leading to increased vitamin D activation through 1-alpha hydroxylase. However, FGF23 acts on the receptor complex in the parathyroid glands to decrease parathyroid hormone gene expression and PTH secretion<sup>46</sup>.

FGF23 also acts on its receptor complex Klotho-FGFR1c in the kidney to repress renal phosphorus reabsorption and suppress the renal synthesis of 1,25(OH)2D<sup>46</sup>. We reported in this study that serum Pi level is normal in SCD at 6 months of age, but there is significantly increased urine Pi/urine creatinine. Higher serum FGF23 levels in SCD mice observed in this study may lead to decreased PTH and therefore decreased serum calcium in SCD mice. Low serum levels of PTH and high serum FGF23 in the SCD group decreases the stimulatory action of PTH on 1 alpha hydroxylase. However, in a hypocalcemic animal, activity of the 1 $\alpha$ -hydroxylase is markedly elevated<sup>47</sup>. These counter-regulatory mechanisms may explain the observation that serum 1,25(OH)2D levels are essentially the same in SCD-IgG and Control-IgG mice.

Studies have shown that several factors are involved in bone metabolism alteration in patients with hemoglobinopathies such as SCD<sup>45</sup>. Among them are bone marrow hyperplasia and increased bone turnover. Bone metabolism reflects an imbalance between bone deposition and bone resorption by osteoblasts and

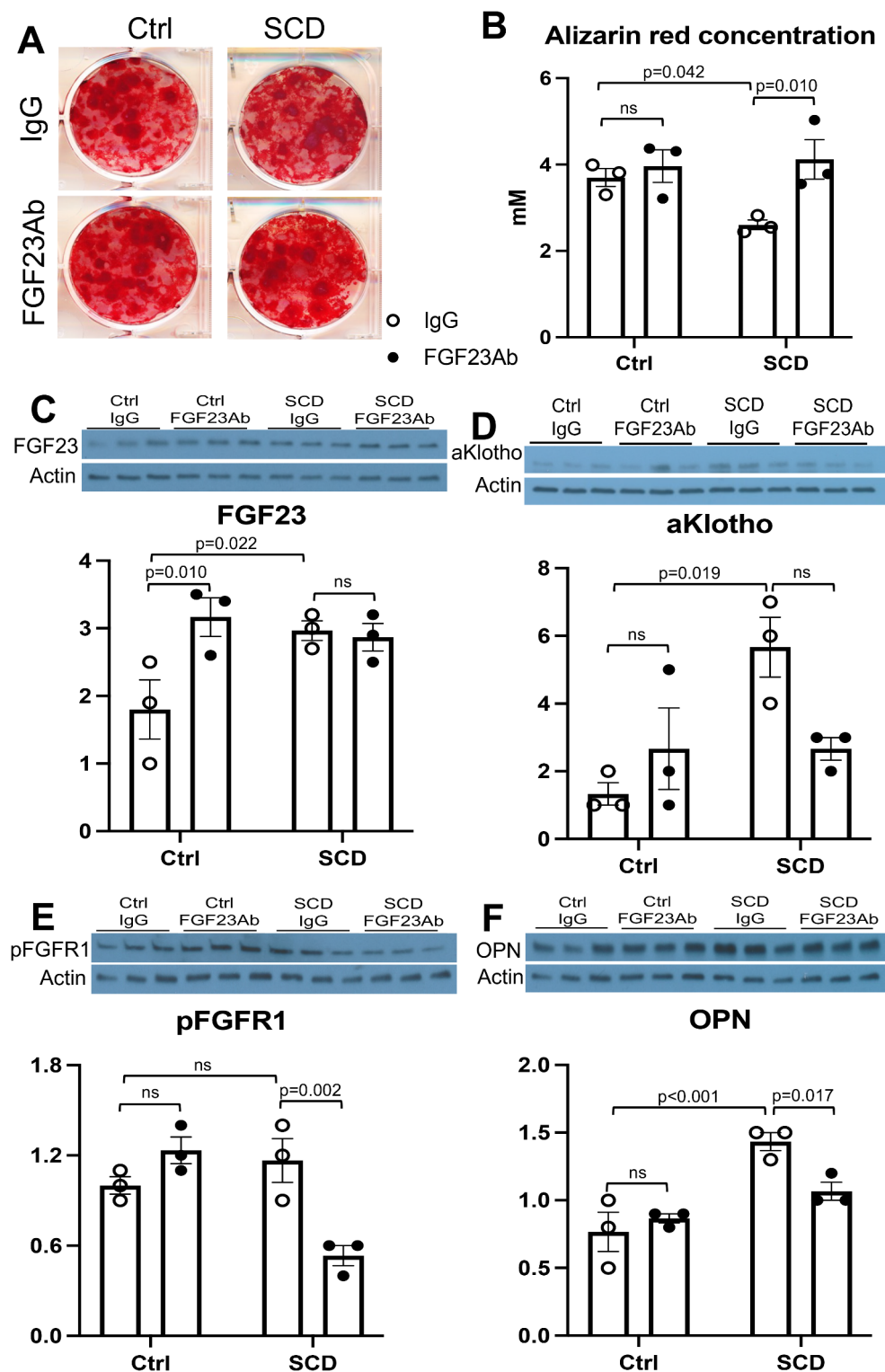


**Fig. 5.** Effect of FGF23Ab on mineralized nodule formation in cultured BMSCs from Ctrl and SCD female mice. Analysis of bone nodule formation and FGF23, pFGFR1 and OPN protein expression in BMSCs from Ctrl and SCD mice. BMSCs from both genotypes were cultured with IgG or FGF23Ab under osteogenic condition for 3 weeks. (A) Representative image of Alizarin Red-staining on 3-weeks culture. (B) Alizarin Red concentration was quantified after solubilization of the staining dye. Western blot and analysis of protein for (C) FGF23, (D) aKlotho, (E) pFGFR1, and (F) Osteopontin;  $n=3$  wells/group. Data are shown as individual values, with mean and standard error of the mean.



osteoclasts that can result in bone diseases, such as osteoporosis<sup>45</sup>. Thus, we examined the changes in bone parameters as determined by DXA, microCT, and dynamic and static histomorphometry. DXA analysis confirmed significantly decreased BMD and BMC in SCD female mice as we previously reported<sup>7</sup> but there was no effect of FGF23Ab treatment to modulate these parameters. The microCT studies did not demonstrate significant differences in femur metaphyseal structural parameters by genotype or treatment. However, von Kossa staining showed markedly increased bone spicule number in the SCD femur after FGF23Ab treatment. This difference between histology and microCT can arise due to several factors: (1) Histomorphometry typically analyzes 2D sections, which may not fully represent 3D bone architecture, whereas  $\mu$ CT provides volumetric data. (2) Thresholding differences:  $\mu$ CT relies on grayscale intensity thresholds to differentiate bone from soft tissue, which may not perfectly match the bone regions identified in histology. MicroCT analysis of femur diaphyseal cortical parameters revealed significantly decreased Ct.Ar, Ct.Ar/Tt.Ar, Ct.Th, and BMD, as well as significantly increased Ma.Ar, all consistent with our previous findings in SCD female mice<sup>7</sup>, but these abnormalities were not modulated by FGF23Ab treatment. However, importantly, dynamic histomorphometry revealed that FGF23Ab treatment of SCD mice significantly increased MAR, BFR/BS, and Ir.L.Th in femurs from SCD mice. We observed that FGF23Ab treatment increased BFR by histomorphometry but did not increase BV/TV by microCT in SCD mice. The possible reason is that BFR by histomorphometry measures ongoing bone formation, while BV/TV by microCT reflects accumulated bone mass over time. MicroCT may not detect early or subtle changes that were detected by histomorphometry. Thus, based on the dynamic histomorphometry results, it is possible that longer FGF23Ab treatment may lead to improvement at the structure level.

It should also be noted that the FGF23Ab used in this study was previously used by Shaloub et al.<sup>48</sup> to investigate the effect of FGF23 neutralization on chronic kidney disease-mineral and bone disorder (CKD-MBD), secondary hyperparathyroidism (HPT), and associated comorbidities in a rat model of CKD-MBD. For these studies, CKD-MBD rats were fed a high-phosphate diet and were treated with low (3 mg/kg) or high doses (10 mg/kg) of FGF23-Ab or an isotype control antibody 3 times/week for 6 weeks. The authors reported that neutralization of FGF23 led to sustained reductions in secondary HPT, and normalization of bone markers such as cancellous bone volume, trabecular number, osteoblast surface, osteoid surface, and bone-formation rate. In addition, they observed dose-dependent increases in serum phosphate and aortic calcification associated with increased risk of mortality in CKD-MBD rats treated with the higher dose of FGF23-Ab. There are several notable differences in our study design using the same antibody in Ctrl and SCD mice. Specifically, we used mice while the previous study used rats. In addition, unlike the rat study, mice were not in chronic renal failure as reflected by the normal blood urea nitrogen (BUN) and creatinine. Further, mice were not on a high phosphate diet, did not exhibit HPT, and the frequency of the administration of the FGF23Ab was less.

Static histomorphometry showed that Oc.S/BS, N.Oc/B.Pm, and N.Oc/T.Ar were significantly higher in the SCD-IgG group vs. the Ctrl-IgG group. FGF23Ab significantly decreased N.Oc/B.Pm in the SCD-FGF23Ab group, which is contradictory to serum CTX1 data showing a significant increase in serum CTX1 levels in FGF23Ab-treated SCD mice. Since serum CTX1 levels have a circadian rhythm which is mainly modulated by food intake, it is recommended that blood samples for CTX1 must be collected consistently in the morning hours in the fasted state<sup>49</sup>. Since fasting can increase the risk of a sickle cell crisis due to potential dehydration, in this study the mice were not fasted. This may explain the inconsistency between N.Oc/B.Pm and serum CTX1 levels.

Since our dynamic histomorphometry studies supported impaired bone formation as the major cause of bone abnormality in SCD mice, to further explore the role of osteoblast dysfunction, we conducted *in vitro* studies demonstrating impaired SCD-BMSC mineralized nodule formation that was rescued by FGF23Ab supporting either a direct<sup>23,24</sup> or indirect<sup>50</sup> inhibitory effect of FGF23 on mineralized bone nodule formation. In support of other inhibitors of mineralization in SCD, we observed significantly increased serum levels of matrix protein osteopontin, which is produced by several tissues including bone<sup>50</sup>. Studies have demonstrated that osteopontin inhibits the proliferation and differentiation of OBs and inhibits mineral deposition in bone<sup>50–52</sup> and is associated with osteoporosis in humans<sup>50</sup>. Of relevance, a recent study by Batte et al. reported on significantly increased serum osteopontin in SCD patients<sup>21</sup> associated with mineral bone disorder. Thus, we determined, in addition to increased serum levels, whether local production of osteopontin was increased in OBs on the bone surface or cultured BMSCs from SCD mice. Since we observed a significant increase in osteopontin protein in OBs on the bone surface and in SCD-IgG BMSC cultures, and this protein was significantly decreased by FGF23Ab treatment, we propose that increased local osteoblast production of osteopontin may contribute to impaired bone formation and mineralization in SCD mice.

We observed that FGF23Ab decreased osteopontin in osteoblasts of bone but not in serum of SCD mice. This discrepancy could reflect differences between local and systemic effects. Possible reasons might be (1) If the treatment directly targets the local bone, changes may appear more prominently in that area, whereas systemic effects may take longer to exhibit differences; (2) The serum detection might not be sensitive enough to capture subtle changes in localized regions, whereas local bone measurements are more precise in identifying these differences. This suggests that the treatment may primarily act locally or that the systemic effects may take longer to manifest.

Based on the results from the current study and our previous publication<sup>53</sup>, we believe FGF23Ab can exert its effects on bone in SCD mice through multiple mechanisms. The *in vitro* study showing FGF23Ab significantly increased bone nodule formation in SCD BMSC culture suggests FGF23Ab can directly affect osteoblast activity. In addition to reduction of the increased matrix inhibitory protein osteopontin by FGF23Ab treatment in SCD mice *in vivo* and *in vitro*, our *in vivo* study showed that FGF23Ab also ameliorates abnormal renal phosphate handling in SCD mice<sup>53</sup> indicating that FGF23Ab can also modulate sickle cell bone loss indirectly via regulating renal phosphate wasting. In SCD, chronic anemia leads to increased erythropoiesis, expanding the bone marrow

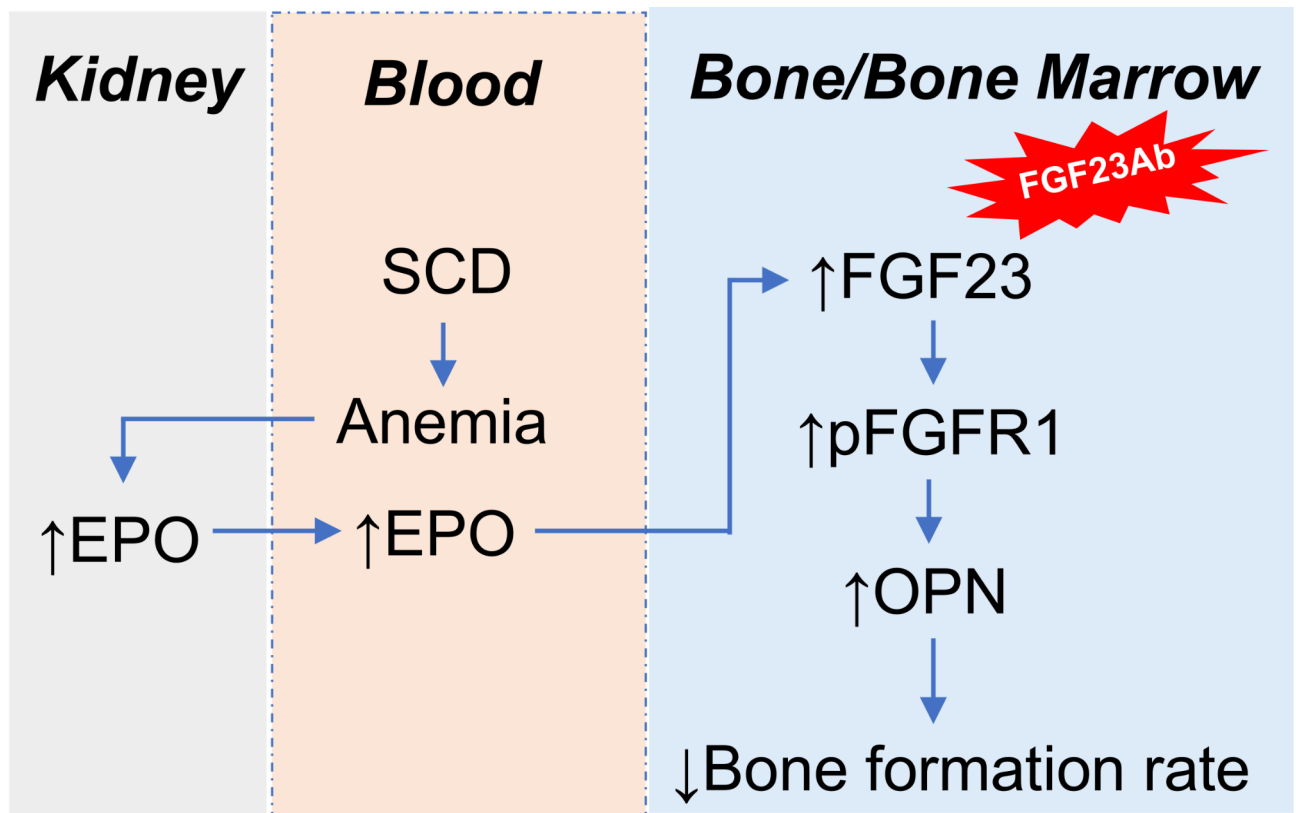


**Fig. 6.** Schematic model depicting how FGF23Ab ameliorate impaired bone formation in SCD mice. In SCD mice, EPO production in the kidneys is increased in response to anemia. High level of EPO circulates to bone to stimulate FGF23 over production that results in impaired bone formation. FGF23Ab ameliorate impaired bone formation in SCD mice by inhibiting FGF23/pFGFR1/OPN pathway.

cavity at the expense of trabecular bone. However, FGF23Ab treatment of SCD mice increased HCT levels, which in turn could improve bone formation by creating a more favorable bone formation niche.

The findings from this study have significant translational potential, as the use of FGF23Ab treatment in the SCD mouse model shows promising results in both increasing hematocrit levels and enhancing bone formation. By targeting FGF23, a key regulator of phosphate metabolism, this approach addresses not only the hematological aspects of SCD but also the associated bone pathology, which is often exacerbated by chronic anemia. The ability to improve both bone formation and hematocrit levels opens new therapeutic avenues for managing osteoporosis and bone deformities in SCD patients. Furthermore, this strategy could be translated to other conditions where both hematopoiesis and bone health are compromised, providing a potential dual-target therapy with broader clinical implications.

In summary, we suggest that FGF23-neutralizing antibody may be efficacious in treating impaired bone formation in SCD based on improvements in osteoblast activity due to improved hematocrit and correction of anemia, which results in the increased bone dynamic histomorphometric parameters observed in FGF23Ab-treated SCD mice and the significant reduction in matrix inhibitory protein osteopontin observed in FGF23Ab-treated BMSC cultures (Fig. 6). Since no effective therapy for SCD bone disease is currently available<sup>54</sup>, these results may inform future studies of FGF23Ab as a therapeutic target for SCD.

### Data availability

Data is provided within the manuscript or supplementary information files. All datasets generated during and/or analyzed during the current study are not publicly available but are available from the corresponding author on reasonable request. The reagents used in this study, Control IgG and a rat anti-rat FGF23Ab (clone 58.5) were a gift from Amgen Inc., Thousand Oaks, CA).

Received: 4 February 2025; Accepted: 20 March 2025

Published online: 28 March 2025

### References

1. Sundd, P., Gladwin, M. T. & Novelli, E. M. Pathophysiology of sickle cell disease. *Annu. Rev. Pathol.* **14**, 263–292. <https://doi.org/10.1146/annurev-pathmechdis-012418-012838> (2019).

2. Sarrai, M., Duroseau, H., D'Augustine, J., Moktan, S. & Bellevue, R. Bone mass density in adults with sickle cell disease. *Br. J. Haematol.* **136**, 666–672. <https://doi.org/10.1111/j.1365-2141.2006.06487.x> (2007).
3. Miller, R. G. et al. High prevalence and correlates of low bone mineral density in young adults with sickle cell disease. *Am. J. Hematol.* **81**, 236–241. <https://doi.org/10.1002/ajh.20541> (2006).
4. Arlet, J. B. et al. Relationship between vitamin D deficiency and bone fragility in sickle cell disease: a cohort study of 56 adults. *Bone* **52**, 206–211. <https://doi.org/10.1016/j.bone.2012.10.005> (2013).
5. Steer, K., Stavrichuk, M., Morris, M. & Komarova, S. V. Bone health in patients with hematopoietic disorders of bone marrow origin: systematic review and Meta- analysis. *J. Bone Min. Res.* **32**, 731–742. <https://doi.org/10.1002/jbmr.3026> (2017).
6. Ryan, T. M., Ciavatta, D. J. & Townes, T. M. Knockout-transgenic mouse model of sickle cell disease. *Science* **278**, 873–876. <https://doi.org/10.1126/science.278.5339.873> (1997).
7. Xiao, L. et al. Loss of bone in sickle cell trait and sickle cell disease female mice is associated with reduced IGF-1 in bone and serum. *Endocrinology* **157**, 3036–3046. <https://doi.org/10.1210/en.2015-2001> (2016).
8. Rana, K., Pantoja, K. & Xiao, L. Bone marrow neutrophil aging in sickle cell disease mice is associated with impaired osteoblast functions. *Biochem. Biophys. Res. Commun.* **16**, 110–114. <https://doi.org/10.1016/j.bbrep.2018.10.009> (2018).
9. Tavakoli, S. & Xiao, L. Depletion of intestinal Microbiome partially rescues bone loss in sickle cell disease male mice. *Sci. Rep.* **9**, 8659. <https://doi.org/10.1038/s41598-019-45270-4> (2019).
10. Dalle Carbonare, L. et al. Hypoxia-reperfusion affects osteogenic lineage and promotes sickle cell bone disease. *Blood* **126**, 2320–2328. <https://doi.org/10.1182/blood-2015-04-641969> (2015).
11. Green, M. et al. Microarchitectural and mechanical characterization of the sickle bone. *J. Mech. Behav. Biomed. Mater.* **48**, 220–228. <https://doi.org/10.1016/j.jmbbm.2015.04.019> (2015).
12. Perwad, F., Zhang, M. Y., Tenenhouse, H. S. & Portale, A. A. Fibroblast growth factor 23 impairs phosphorus and vitamin D metabolism in vivo and suppresses 25-hydroxyvitamin D-1 $\alpha$ -hydroxylase expression in vitro. *Am. J. Physiol. Ren. Physiol.* **293**, F1577–F1583. <https://doi.org/10.1152/ajprenal.00463.2006> (2007).
13. Shimada, T. et al. FGF-23 is a potent regulator of vitamin D metabolism and phosphate homeostasis. *J. Bone Min. Res.* **19**, 429–435. <https://doi.org/10.1359/JBMR.0301264> (2004).
14. Clindenbeard, E. L. et al. Erythropoietin stimulates murine and human fibroblast growth factor-23, revealing novel roles for bone and bone marrow. *Haematologica* **102**, e427–e430. <https://doi.org/10.3324/haematol.2017.167882> (2017).
15. Daryadel, A. et al. Erythropoietin stimulates fibroblast growth factor 23 (FGF23) in mice and men. *Pflugers Arch.* **470**, 1569–1582. <https://doi.org/10.1007/s00424-018-2171-7> (2018).
16. Zhang, Q. et al. The hypoxia-inducible factor-1 $\alpha$  activates ectopic production of fibroblast growth factor 23 in tumor-induced osteomalacia. *Bone Res.* **4**, 16011. <https://doi.org/10.1038/boneres.2016.11> (2016).
17. Jonsson, K. B. et al. Fibroblast growth factor 23 in oncogenic osteomalacia and X-linked hypophosphatemia. *N. Engl. J. Med.* **348**, 1656–1663. <https://doi.org/10.1056/NEJMoa020881> (2003).
18. Yamashita, T., Yoshioka, M. & Itoh, N. Identification of a novel fibroblast growth factor, FGF-23, preferentially expressed in the ventrolateral thalamic nucleus of the brain. *Biochem. Biophys. Res. Commun.* **277**, 494–498. <https://doi.org/10.1006/bbrc.2000.3696> (2000).
19. Raj, V. M. et al. Abnormalities in renal tubular phosphate handling in children with sickle cell disease. *Pediatr. Blood Cancer.* **61**, 2267–2270. <https://doi.org/10.1002/pbc.25188> (2014).
20. Courbebaisse, M. et al. Carboxy-terminal fragment of fibroblast growth factor 23 induces heart hypertrophy in sickle cell disease. *Haematologica* **102**, e33–e35. <https://doi.org/10.3324/haematol.2016.150987> (2017).
21. Batte, A. et al. Mineral bone disorders and kidney disease in hospitalized children with sickle cell anemia. *Front. Pediatr.* **10**, 1078853. <https://doi.org/10.3389/fped.2022.1078853> (2022).
22. Millington, G. et al. Fibroblast growth factor 2 high molecular weight isoforms in Dentoalveolar mineralization. *Calcif Tissue Int.* **110**, 93–103. <https://doi.org/10.1007/s00223-021-00888-3> (2022).
23. Xiao, L., Eslinger, A. & Hurley, M. M. Nuclear fibroblast growth factor 2 (FGF2) isoforms inhibit bone marrow stromal cell mineralization through FGF23/FGFR/MAPK in vitro. *J. Bone Min. Res.* **28**, 35–45. <https://doi.org/10.1002/jbmr.1721> (2013).
24. Shalhoub, V. et al. Fibroblast growth factor 23 (FGF23) and alpha-klotho stimulate osteoblastic MC3T3.E1 cell proliferation and inhibit mineralization. *Calcif Tissue Int.* **89**, 140–150. <https://doi.org/10.1007/s00223-011-9501-5> (2011).
25. Wang, H. et al. Overexpression of fibroblast growth factor 23 suppresses osteoblast differentiation and matrix mineralization in vitro. *J. Bone Min. Res.* **23**, 939–948. <https://doi.org/10.1359/jbmr.080220> (2008).
26. Aono, Y. et al. Therapeutic effects of anti-FGF23 antibodies in hypophosphatemic rickets/osteomalacia. *J. Bone Min. Res.* **24**, 1879–1888. <https://doi.org/10.1359/jbmr.090509> (2009).
27. Ishii, S. et al. FGF-23 from erythroblasts promotes hematopoietic progenitor mobilization. *Blood* **137**, 1457–1467. <https://doi.org/10.1182/blood.2020007172> (2021).
28. Weidner, H. et al. Increased FGF-23 levels are linked to ineffective erythropoiesis and impaired bone mineralization in myelodysplastic syndromes. *JCI Insight* **5**, 56. <https://doi.org/10.1172/jci.insight.137062> (2020).
29. Rossaint, J. et al. FGF23 signaling impairs neutrophil recruitment and host defense during CKD. *J. Clin. Invest.* **126**, 962–974. <https://doi.org/10.1172/JCI83470> (2016).
30. Insogna, K. L. et al. Burosumab improved histomorphometric measures of osteomalacia in adults with X-Linked hypophosphatemia: a phase 3, Single-Arm, international trial. *J. Bone Min. Res.* **34**, 2183–2191. <https://doi.org/10.1002/jbmr.3843> (2019).
31. Xiao, L., Homer-Bouthiette, C. & Hurley, M. M. FGF23 neutralizing antibody partially improves bone mineralization defect of HMWFGF2 isoforms in Transgenic female mice. *J. Bone Min. Res.* **33**, 1347–1361. <https://doi.org/10.1002/jbmr.3417> (2018).
32. Ma, L., Yang, S., Peng, Q., Zhang, J. & Zhang, J. CRISPR/Cas9-based gene-editing technology for sickle cell disease. *Gene* **874**, 147480. <https://doi.org/10.1016/j.gene.2023.147480> (2023).
33. Sheridan, C. The world's first CRISPR therapy is approved: who will receive it? *Nat. Biotechnol.* **42**, 3–4. <https://doi.org/10.1038/d41587-023-00016-6> (2024).
34. Kanter, J. et al. Biologic and clinical efficacy of lentioglobulin for sickle cell disease. *N. Engl. J. Med.* **386**, 617–628. <https://doi.org/10.1056/NEJMoa2117175> (2022).
35. Goyal, S. et al. Acute myeloid leukemia case after gene therapy for sickle cell disease. *N. Engl. J. Med.* **386**, 138–147. <https://doi.org/10.1056/NEJMoa2109167> (2022).
36. Suresh, S., Rajvanshi, P. K. & Noguchi, C. T. The many facets of erythropoietin physiologic and metabolic response. *Front. Physiol.* **10**, 1534. <https://doi.org/10.3389/fphys.2019.01534> (2019).
37. Zarjou, A. et al. Ferritin ferroxidase activity: a potent inhibitor of osteogenesis. *J. Bone Min. Res.* **25**, 164–172. <https://doi.org/10.1359/jbmr.091002> (2010).
38. Murali, S. K. et al. FGF23 regulates bone mineralization in a 1,25(OH) $_2$ D $_3$  and Klotho-Independent manner. *J. Bone Min. Res.* **31**, 129–142. <https://doi.org/10.1002/jbmr.2606> (2016).
39. Ginzburg, Y. Z. & Glassberg, J. Inflammation, hemolysis, and erythropoiesis lead to competitive regulation of Hepcidin and possibly systemic iron status in sickle cell disease. *EBioMedicine* **34**, 8–9. <https://doi.org/10.1016/j.ebiom.2018.07.023> (2018).
40. Sherwood, J. B., Goldwasser, E., Chilcote, R., Carmichael, L. D. & Nagel, R. L. Sickle cell anemia patients have low erythropoietin levels for their degree of anemia. *Blood* **67**, 46–49 (1986).
41. Agoro, R. et al. Inhibition of fibroblast growth factor 23 (FGF23) signaling rescues renal anemia. *FASEB J.* **32**, 3752–3764. <https://doi.org/10.1096/fj.201700667R> (2018).

42. Pulte, E. D., McKenzie, S. E., Caro, J. & Ballas, S. K. Erythropoietin levels in patients with sickle cell disease do not correlate with known inducers of erythropoietin. *Hemoglobin* **38**, 385–389. <https://doi.org/10.3109/03630269.2014.967868> (2014).
43. Karafin, M. S. et al. Erythropoietic drive is the strongest predictor of Hepcidin level in adults with sickle cell disease. *Blood Cells Mol. Dis.* **55**, 304–307. <https://doi.org/10.1016/j.bcmd.2015.07.010> (2015).
44. Coe, L. M. et al. FGF-23 is a negative regulator of prenatal and postnatal erythropoiesis. *J. Biol. Chem.* **289**, 9795–9810. <https://doi.org/10.1074/jbc.M113.527150> (2014).
45. Di Paola, A. et al. Bone health impairment in patients with hemoglobinopathies: from biological bases to new possible therapeutic strategies. *Int. J. Mol. Sci.* **25**, 23. <https://doi.org/10.3390/ijms25052902> (2024).
46. Silver, J. & Naveh-Many, T. FGF23 and the parathyroid glands. *Pediatr. Nephrol.* **25**, 2241–2245. <https://doi.org/10.1007/s00467-010-1565-3> (2010).
47. Brenza, H. L. et al. Parathyroid hormone activation of the 25-hydroxyvitamin D3-1alpha-hydroxylase gene promoter. *Proc. Natl. Acad. Sci. U. S. A.* **95**, 1387–1391. <https://doi.org/10.1073/pnas.95.4.1387> (1998).
48. Shalhoub, V. et al. FGF23 neutralization improves chronic kidney disease-associated hyperparathyroidism yet increases mortality. *J. Clin. Invest.* **122**, 2543–2553. <https://doi.org/10.1172/JCI61405> (2012).
49. Szulc, P. et al. Use of CTX-I and PINP as bone turnover markers: National bone health alliance recommendations to standardize sample handling and patient Preparation to reduce pre-analytical variability. *Osteoporos. Int.* **28**, 2541–2556. <https://doi.org/10.1007/s00198-017-4082-4> (2017).
50. Si, J., Wang, C., Zhang, D., Wang, B. & Zhou, Y. Osteopontin in bone metabolism and bone diseases. *Med. Sci. Monit.* **26**, e919159. <https://doi.org/10.12659/MSM.919159> (2020).
51. Holm, E. et al. Osteopontin mediates mineralization and not osteogenic cell development in vitro. *Biochem. J.* **464**, 355–364. <https://doi.org/10.1042/BJ20140702> (2014).
52. Huang, W. et al. Osteopontin is a negative regulator of proliferation and differentiation in MC3T3-E1 pre-osteoblastic cells. *Bone* **34**, 799–808. <https://doi.org/10.1016/j.bone.2003.11.027> (2004).
53. Xiao, L., Clarke, K. & Hurley, M. M. Fibroblast growth factor 23 neutralizing antibody ameliorates abnormal renal phosphate handling in sickle cell disease mice. *Endocrinology* **164**, 896. <https://doi.org/10.1210/endo/bqad173> (2023).
54. Maldonado, L. Y. et al. Racial and ethnic disparities in metabolic bone disease. *Endocrinol. Metab. Clin. North. Am.* **52**, 629–641. <https://doi.org/10.1016/j.ecl.2023.05.004> (2023).

## Acknowledgements

This work was supported by National Institutes of Health [grant number R01DK129431-01A1, 2022]. The authors would like to thank the Amgen Inc., (Thousand Oaks, CA) for providing the reagent Control IgG and a rat anti-rat FGF23Ab (clone 58.5) used in the study.

## Author contributions

MMH conceived, coordinated and designed the study and wrote the paper. LX performed, analyzed the experiments shown, and revised the manuscript. WH provided technical assistance. All authors reviewed the results and approved the final version of the manuscript.

## Funding

This work was supported by National Institutes of Health [grant number R01DK129431-01A1, 2022].

## Competing interests

The authors declare no competing interests.

## Additional information

**Supplementary Information** The online version contains supplementary material available at <https://doi.org/10.1038/s41598-025-95335-w>.

**Correspondence** and requests for materials should be addressed to L.X. or M.M.H.

**Reprints and permissions information** is available at [www.nature.com/reprints](http://www.nature.com/reprints).

**Publisher's note** Springer Nature remains neutral with regard to jurisdictional claims in published maps and institutional affiliations.

**Open Access** This article is licensed under a Creative Commons Attribution-NonCommercial-NoDerivatives 4.0 International License, which permits any non-commercial use, sharing, distribution and reproduction in any medium or format, as long as you give appropriate credit to the original author(s) and the source, provide a link to the Creative Commons licence, and indicate if you modified the licensed material. You do not have permission under this licence to share adapted material derived from this article or parts of it. The images or other third party material in this article are included in the article's Creative Commons licence, unless indicated otherwise in a credit line to the material. If material is not included in the article's Creative Commons licence and your intended use is not permitted by statutory regulation or exceeds the permitted use, you will need to obtain permission directly from the copyright holder. To view a copy of this licence, visit <http://creativecommons.org/licenses/by-nc-nd/4.0/>.

© The Author(s) 2025